

CO-CONICAL FIELD GENERATION SYSTEM - A 40 GHz ANTENNA CALIBRATION CELL

David R. Novotny, Arthur Ondrejka, Robert Johnk
National Institute of Standards and Technology
RF Fields Division
325 Broadway
Boulder, Colorado 80303

I. INTRODUCTION:

A prototype test cell for generating standard fields suitable for antenna calibrations from DC to 40 GHz has been developed and tested. A 1 m scale model of the Co-Conical Field Generation System (CFGS), an expanding, constant-impedance coaxial transmission system has been constructed. Symmetry throughout the cell establishes a uniform and calculable wavefront. This symmetry also maintains the dominant TEM mode structure and, more importantly, allows for the gradual and efficient termination of the incident energy. Simple termination schemes have generally provided more than 20 dB absorption of the injected energy, with complex designs showing much more promise. The field structure within the test volume has been mapped by measuring the reflections by a small passive scatterer. The measurement results agree well with transmission line theory and show no significant signs of mode degradation as energy propagates down the cell. Various numerical techniques agree well with the measurement results and transmission line equations, allowing for further study of scattering effects within the cell.

II. HISTORY:

Closed, two-conductor cells have been used for generating standard calibration fields since Crawford popularized the use of the TEM cell [1]. The single-mode nature of a Crawford TEM cell limits the operation to a frequency corresponding to less than a $\lambda/2$ distance between the outer and inner conductors. Recently, use of gigahertz-TEM cells (GTEM) has been expanding. GTEMs operate at higher frequencies; however, their non-symmetric transmission structure and termination schemes can lead to higher-order mode generation and field uniformity issues.

U.S. Government work not subject to copyright. Supported by Air Force CCG - Newark AFB.

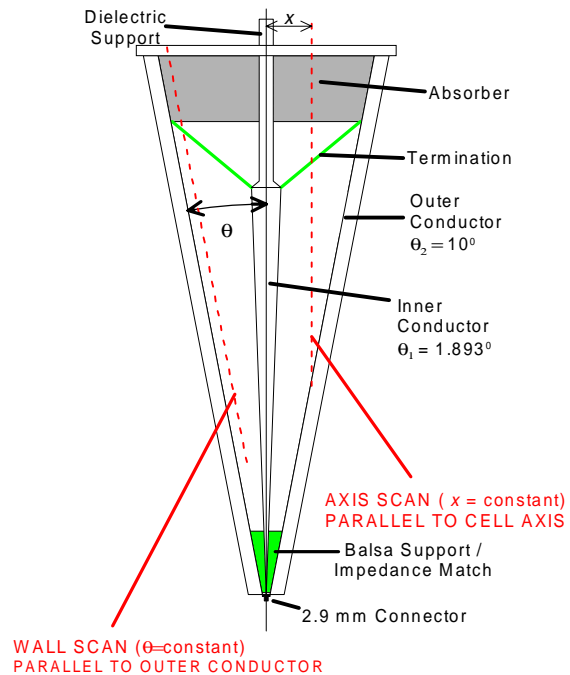


Figure 1 Cross section of the Co-Conical Field Generation System

For over 20 years, the RF Fields Division at NIST has been generating standard fields up to 10 GHz using the “cone and ground plane” method [2] based on the coaxial cone transmission line described by Schelkunoff [3] in 1943. The Co-Conical Field Generation System (Fig. 1) is a closed-cell implementation of the same concept. It is essentially an expanding coaxial line with constant capacitance and impedance. The dominant TEM mode is propagated and higher order modes are not significantly excited by maintaining symmetry in the transmission structure. This same symmetric, single-mode wave allows for a very efficient and gradual termination of the incident energy and cell geometry. The launch of the uniform spherical wave provides an easily calculable field with a known non-uniformity in the test volume.

The CFGS is intended to provide a relatively cost effective method for generating a high quality standard field across a broad bandwidth. While conventional anechoic chambers can provide a larger test volume, they are limited in bandwidth by the horns or power delivery systems, and the costs of equipment and labor for high power, broadband testing are considerable. The CFGS can perform limited-volume testing for considerably less cost than an anechoic chamber. Since the fields are confined within the cell, the radiated power density is greater for a given amplifier, which can allow for the use of lower cost, lower power, broadband amplifiers. These broadband features can lead to significant time savings in calibrations.

II. THEORY AND MODELING

Schelkunoff developed the field and impedance solutions for the coaxial cone transmission line. These generally follow from the analysis of a biconical antenna. The dominant outward bound electric (E) and magnetic (H) fields are

$$E_{\theta} = \frac{\eta_0 P e^{-j\beta r} e^{-j\omega t}}{r \sin \theta}, \quad H_{\phi} = \frac{P e^{-j\beta r} e^{-j\omega t}}{r \sin \theta}, \quad (1)$$

where η_0 is the impedance of free space, r is the distance from the cone feed, and P is the normalized current on the center conductor at the feed point of the cones. If the substitution $\sin(\theta) = x/r$ is made, then (1) becomes,

$$E_{\theta} = \frac{\eta_0 P e^{-j\beta r}}{x}, \quad H_{\phi} = \frac{P e^{-j\beta r}}{x}. \quad (2)$$

The impedance Z_c of the cell follows from the derivation of the normalized current P ,

$$Z_c = \frac{\eta_0}{2\pi\sqrt{\epsilon_r}} \ln \left(\cot \left(\frac{\theta_1}{2} \right) \tan \left(\frac{\theta_2}{2} \right) \right), \quad (3)$$

where ϵ_r is the relative permittivity of the material between the conductors, θ_1 is the half angle of the inner cone, and θ_2 is the half angle of the outer cone.

Equation (2) shows that for the lossless case, the field *amplitudes* are a function only of the lateral distance from the cone axis x (Fig. 2). This leads to not spherical or conical, but *cylindrical field contours within the cell*. This means positioning of an artifact under test (AUT) depends on distance from the central axis and not the distance from the feed. This allows for less critical positioning of the AUT within the test

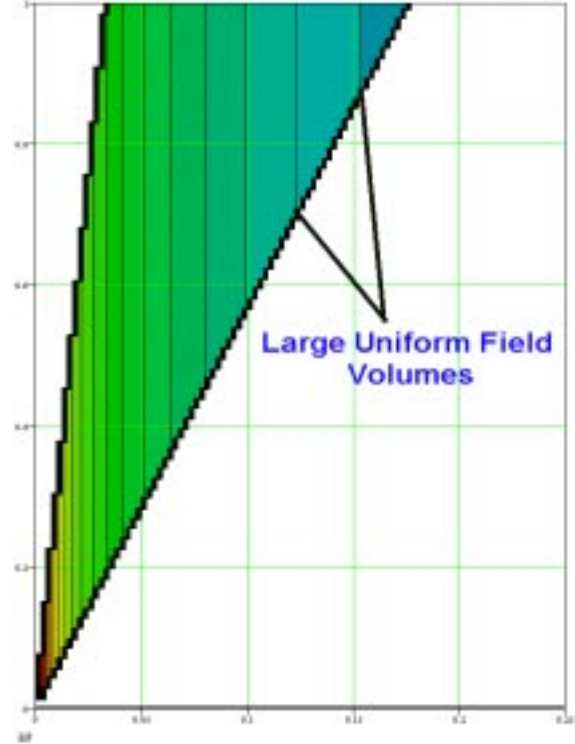


Figure 2. Analytic field amplitude distribution. Shows cylindrical structure of the electric fields.

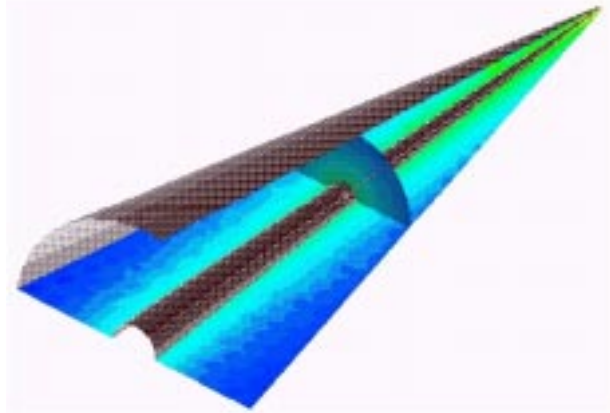


Figure 3. Finite element simulation of the fields within the CFGS. Field structures mirror the analytic solution.

volume, which may reduce position-dependent uncertainties.

The closed form field results were compared with a simulation using a finite element solver. Figure 3 shows the results for a 50Ω cable feeding a 100Ω cell. Both solutions show the same cylindrical field contours and similar field tapers as a function of lateral position. These results form a baseline for future modeling of the termination and scatterers within the system.

III. TERMINATION DESIGN

The 1 m test cell is shown in Figure 1. A cell impedance of $Z_c=100\ \Omega$ was chose, leading to $\theta_2 = 10^\circ$ and $\theta_1 \approx 1.893^\circ$. This resulted in a practical test volume and made the center conductor a small enough mass to handle. The single-stage termination was constructed from a commercially available radar-absorbing cloth with broadband absorption characteristics and a stable DC conductivity. This material was affixed to a thin vinyl cone which made contact with both conductors. The cone (Fig. 4) was constructed so that the termination and outer cone met in a geometrical Brewster's angle to reduce reflections. Behind the thin termination material, a urethane absorber was placed to absorb energy transmitted through the termination and reduce any reflections from behind the termination.



Figure 4. CFGS $100\ \Omega$ termination with probe slot

A time domain reflectometry (TDR) study of the cell was performed with a 24 GHz pulsed step generator/oscilloscope and a 40 GHz vector network analyzer (VNA). The TDR showed the impedance stayed within $1\ \Omega$ of the designed $Z_c = 100\ \Omega$ throughout the transmission volume. The termination impedance also stayed within $10\ \Omega$ of the desired $100\ \Omega$ value from 10 MHz to 40 GHz. When viewed in the frequency domain (Fig. 5), the reflection from the termination is less than $-20\ \text{dB}$, except in the 2-5 GHz range, which is directly attributable to poor connections between the termination and center and outer conductors. This is being rectified in newer designs.

IV. FEED DESIGN

The quality of the field in the test volume is extremely dependent on the field structure at the feed point of the cell, a great deal of effort was put into improving the feed and structure of the fields launched into the cell. Initially the cone was suspended in free space and centered with a foam insert. This arrangement lacked the structural rigidity required for a full scale cell and a

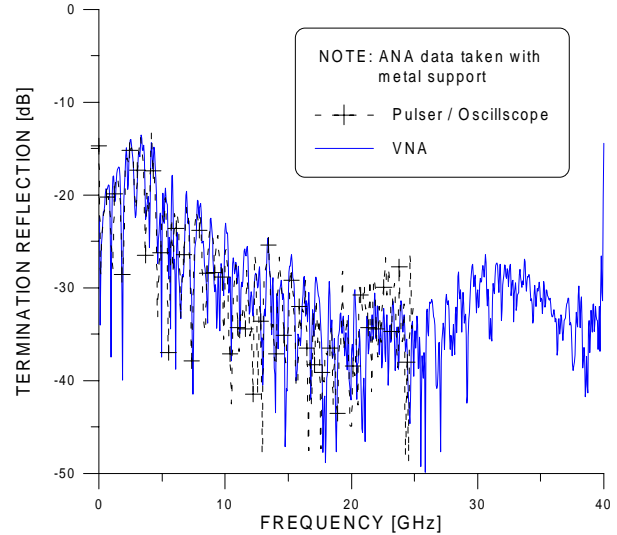


Figure 5. Termination performance within the CFGS.

rigorous testing environment. By slightly increasing θ_2 and filling the feed with an appropriate dielectric constant, ϵ_r . The impedance of the cell can be maintained and the dielectric can support and align the center conductor.

In the first 66 mm section of the CFGS, θ_2 was manufactured at approximately 10.8° . With $\theta_1 = 1.893^\circ$ this yielded an initial impedance of $104.7\ \Omega$ before settling down to the $Z_0=100\ \Omega$ of the rest of the cell. A dense foam insert ($\epsilon_r=1.05$) reduced the impedance to approximately $102\ \Omega$ and a solid balsa wood insert ($\epsilon_r \approx 1.25$) reduced the impedance to roughly $95\ \Omega$. The impedance was raised to approximately $98\ \Omega$ by drilling radially symmetric, stepped holes in the balsa insert. Using these results, we conclude that with an initial $\theta_2 = 11.7^\circ$ and an appropriate dielectric insert, a feed structure can be made to maintain the impedance of the cell and have the strength required to support the center conductor.

V. FIELD UNIFORMITY STUDIES

Ultimately, the usefulness of the CFGS will be determined by its field uniformity. A passive scattering technique was employed to measure the electric field at discrete points within the test volume. The concept of measuring field distributions within waveguides and free space by using a passive or modulated scatterer has been in the literature for over 40 years [4]. The reflected voltage received from a small scatterer is proportional to the square of the electric field at the point of the scatterer. A direct measurement of the

fields and field uniformity can be made by moving a scatterer through the volume of the CFGS. We moved a small cylindrical scatterer (radius = 0.26 mm, length = 10 mm) along the wall of the cell (Fig. 1: wall scan) and along a constant $x = 60$ mm path (axis scan). The scatterer was aligned in the θ direction to give maximum response to the E_θ field component. The 50 Ω to 100 Ω interface was mathematically removed by background subtraction. The resulting difference left only the reflections from the scatterer.

The wall scans generally agreed with theory within ± 1 dB as the scatterer traveled over a 63 cm distance. Figure 6 shows the difference between the theoretical and measured normalized fields as the scatterer is moved toward the feed. There were no signs of higher order modes, which would be manifested as cyclic variations as a function of position or frequency. The axis scans (Fig. 7) showed the cylindrical field contours. The theoretically constant field was flat to generally within ± 2 dB over a 35 cm scan distance. As the probe neared the feed some excursions as high as 4 dB were noted; however, these could be due to positioning errors since the scatterer was in its most distant point from its support. The axis scans have larger variations which can be due to positioning errors. In the axis scans, the probe was suspended by a thin (1 mm) balsa slab in the middle of the cell. By contrast, during the wall scans the scatterer was always supported by the cell wall.

The field scans show that the dominant TEM mode was preserved up to the termination. The axis scan also

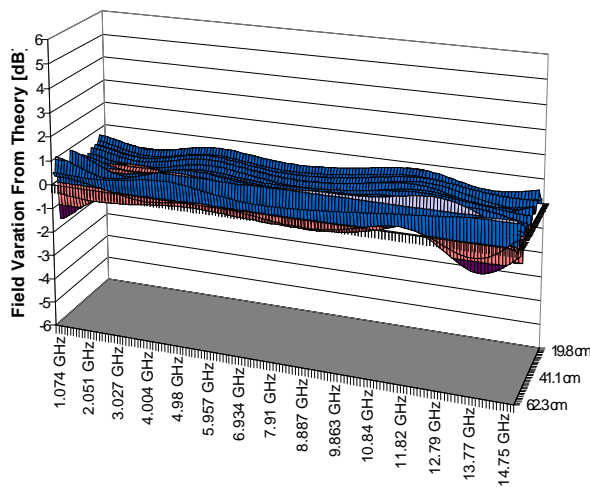


Figure 6. Wall scan 1-16 GHz. Results normalized to theoretical $1/r$ dependence.

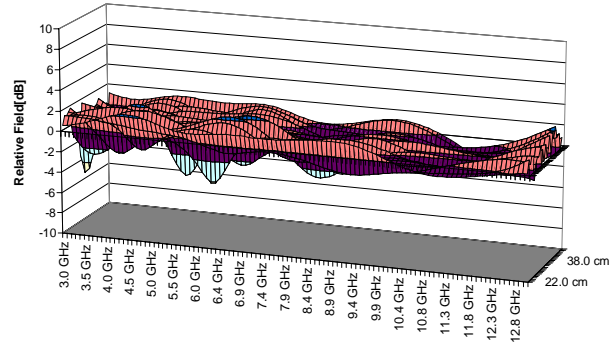


Figure 7. Axis Scan $x=60$ mm. Amplitude is generally flat to within ± 2 dB.

indicates that the transmission losses were fairly small. The lack of significant loss over frequency and position suggest that a larger cell should have limited field nonuniformities due to ohmic losses in the system.

VI. CONCLUSION

A quality calibration field in a confined test volume can be generated. The 1 m CFGS has shown that a single-mode field can be generated, transmitted, and absorbed over a broad band of frequencies. The fields are easily calculable, and the cylindrical field contours give a relatively easy method for positioning an AUT within the cell. Some practical design concepts such as a viable termination and a realistic center conductor support have been demonstrated. The CFGS can be a practical alternative to an anechoic chamber for testing small devices.

[1] M. L. Crawford, "Generation of Standard EM Fields Using TEM Transmission Cells," IEEE Transactions on Electromagnetic Compatibility, vol. EMC-16(4), pp.189-195, Nov. 1974.

[2] R. A. Lawton, A. R. Ondrejka, "Antennas and the Associated Time Domain Range for the Measurement of Impulsive Fields," National Bureau of Standards (U.S.) Technical Note 1008, Nov. 1978.

[3] S. A. Schelkunoff, "Electromagnetic Waves," D. Van Nostrand Company, Inc., New York, N.Y., pp. 285-289, 1943.

[4] R. Justice and V. H. Rumsey, "Measurement of Electric Field Distributions," IRE Transactions on Antennas and Propagation, vol. AP-3, no. 4, pp. 177-180, Oct. 1955.